International Journal of Fracture (2005) 131:L37–L44
DOI 10.1007/s10704-004-0020-5

AGGLOMERATION AND REFRAGMENTATION IN MICROSCALE GRANULAR FLOWS

I. Temizer and T. I. Zohdi
Department of Mechanical Engineering
6195 Etcheverry Hall
University of California, Berkeley, CA, 94720-1740, USA
email: temizeil or zohdi@me.berkeley.edu, fax. 510-642-5539

Abstract. A model is developed to describe dendritic agglomeration in microscale granular flows. The individual particulate grains under consideration are approximated as being spheres that remain spherical after impact. The spheres may adhere to one another, forming branched aggregates ("dendrites"), based upon an empirical contact pressure relation. The possibility for fragmentation is also included in the analysis. The computational model developed is used to demonstrate agglomeration behavior in granular flows for a range of control parameters. The results indicate that there is a transition from size-unstable agglomeration to size-stable agglomeration, which is controlled by the velocity field and the material properties.

1. Introduction. A popular theory for planet formation argues that mechanically and electrically induced aggregation [1] of dust, ice and rock particles in a gaseous medium results in particulate growth, leading to critical sizes, so-called planetesimals, where gravitational forces may then dominate. This mixture of particles and gas are loosely referred to as a protoplanetary disk, and represents a type of granular material. In a purely mechanical setting the driving mechanism for aggregation is impact and adhesion. If the colliding aggregates are small, then the possible outcome of the collision is either that they will adhere and agglomerate (through chemical and mechanical bonds) or rebound. In certain cases, it is necessary to take into account fragmentation or debonding among adhered particles of agglomerates involved in the collision. For small particle sizes, mechanical bonding and electrostatic attraction forces are dominant for aggregation, while for large bodies gravitation is the driving force for aggregation [Weidenschilling et al., 1997]. In order to isolate the purely mechanical effects, neither of these effects will be addressed in this work.

For algorithmic and experimental aspects of particle agglomeration, the interested reader is referred to Richardson et al. [2000] and Blum and Wurm [2000], respectively. Problems of adhesion and restructuring of aggregates were addressed by Dominik and Tielens [1997], where the authors took into account electrical attraction/repulsion forces between particles. Sirono and Greenberg [2000] presented mechanical aspects of restructuring, such as tensile and compressive strengths of aggregates. A detailed mechanical analysis can be found in the paper by Chokshi et al. [1993], where the authors investigated impact, adhesion, restructuring of colliding dust particles, as well as topological (particle shape) and tribological (surface roughness) aspects. Specifically, fragmentation after collisions was modeled by Benz [1994]. Effects of the presence

[1] The terms aggregation/agglomeration and aggregate/agglomerate will be used interchangeably.

of surrounding fluid were investigated by Wurm et al. [2001]. The Cosmic Dust Aggregation Experiment (CODAG) of Jena University, Germany, investigated particle agglomeration physics through microgravity experiments. For a detailed review of the CODAG experiments, the reader is referred to Huijser et al. [1999]. In Zohdi

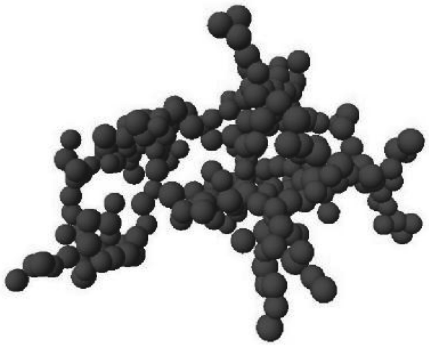

Figure 1: A branched aggregate from a numerical experiment in this work.

[2003], a model for the aggregation for such granular material flows was developed. Although this model included thermo-chemical effects, it assumed self-similar growth, i.e. spherical particles would grow into larger spherical particles. This does not adequately describe aggregates such as those found in CODAG experiments. Therefore, the present work, while neglecting thermo-chemistry, attempts to correct this deficiency by allowing for branched ("dendritic" or "chain-like") growth (Figure 1). The individual particulate grains under consideration are approximated as being spheres that remain spherical after impact. The spheres may adhere to one another, forming branched aggregates ("dendrites"), based upon an empirical contact pressure relation. The possibility for fragmentation is also included in the analysis. Recently in Zohdi [2004(a] and Zohdi [2004(b], models for agglomeration due to thermo-chemical and electrical effects were developed that can describe such growth.

2. Impact. Consider impact, with friction, of two aggregates of spheres of arbitrary shape, denoted A_1 and A_2, in three dimensions. The following assumptions are made: (i) restructuring of the aggregates takes place after they attain their final post-impact velocities, (ii) the impact duration is much smaller than the computational time step used, (iii) the changes in the positions of all spheres in the impact duration are negligibly small, (iv) the spheres are assumed to remain spherical after impact, (v) the forces involved in the calculations are only those that result from the impact, (vi) the deformations sustained by the aggregates due to inertial forces are negligibly small. Suppose contact of the two aggregates occurs at point C, between sphere s_1 of A_1 and sphere s_2 of A_2. A vector $\boldsymbol{n}$ is defined to be the unit vector that points from the center of s_1 to the center of s_2: $\boldsymbol{n} = \frac{\boldsymbol{r}_2 - \boldsymbol{r}_1}{\|\boldsymbol{r}_2 - \boldsymbol{r}_1\|}$. The position $\boldsymbol{R}_i^c$ of point C with respect to the aggregates is calculated by $\boldsymbol{R}_i^c = \boldsymbol{r}_i + r_i \boldsymbol{n}$, where r_i is the radius of sphere s_i and $\boldsymbol{r}_i$ is the position of sphere s_i. The velocities at point C, denoted by $\boldsymbol{V}_i^c$, are given by $\boldsymbol{V}_i^c = \boldsymbol{V}_i + \boldsymbol{\Omega}_i \times \boldsymbol{R}_i^c$, where $\boldsymbol{R}_i^c$ is the position of C with respect to

center of mass, $\boldsymbol{V}_i$ is the center of mass velocity and $\boldsymbol{\Omega}_i$ is the angular velocity of A_i. The coefficient of restitution, e, is then defined as

$$e = \frac{(V_2^c)_{nor}^{(t+\delta t)} - (V_1^c)_{nor}^{(t+\delta t)}}{(V_1^c)_{nor}^{(t)} - (V_2^c)_{nor}^{(t)}} \tag{1}$$

where $(V_i^c)_{nor} = (\boldsymbol{V}_i + \boldsymbol{\Omega}_i \times \boldsymbol{R}_i^c) \cdot \boldsymbol{n}$, t denotes impact time and δt is the impact duration. When there is frictional interaction, it is useful to define $\boldsymbol{t}_1 = \frac{(\boldsymbol{V}_1^c)^{(t)} - (\boldsymbol{V}_2^c)^{(t)}}{\left|(\boldsymbol{V}_1^c)^{(t)} - (\boldsymbol{V}_2^c)^{(t)}\right|}$ and $\boldsymbol{t}_2 = \boldsymbol{n} \times \boldsymbol{t}_1$, so that $\boldsymbol{t}_1$ points in the direction of sliding. Since there is no interaction at the contact point in the direction $\boldsymbol{t}_2$, one has

$$M_1 \boldsymbol{V}_1^{(t)} \cdot \boldsymbol{t}_2 = M_1 \boldsymbol{V}_1^{(t+\delta t)} \cdot \boldsymbol{t}_2 \quad . \tag{2}$$

The frictional interaction is incorporated by the equation

$$M_1 \boldsymbol{V}_1^{(t)} \cdot \boldsymbol{t}_1 + F_f = M_1 \boldsymbol{V}_1^{(t+\delta t)} \cdot \boldsymbol{t}_1 \quad , \tag{3}$$

where $F_f = \mu M_1 \left((\boldsymbol{V}_1)^{(t+\delta t)} - (\boldsymbol{V}_1)^{(t)} \right) \cdot \boldsymbol{n}$ is the frictional impulse along the direction of sliding and μ is the friction coefficient.

The position $\boldsymbol{C}_i$ of the center of mass of a body with respect to contact point C is defined by $\boldsymbol{C}_i = -\boldsymbol{R}_i^c$. It is assumed that the variation in the magnitude and direction of $\boldsymbol{C}_i$ for the two aggregates involved in impact is negligibly small. It is also assumed that the force distribution over the contact surface generates no moments about point C. It follows that the angular momentum $\boldsymbol{H}_i^c$ for each body about point C is conserved during impact: $(\boldsymbol{H}_i^c)^{(t+\delta t)} = (\boldsymbol{H}_i^c)^{(t)}$. Therefore, the following equations are obtained for the aggregates involved in impact:

$$\begin{aligned} \boldsymbol{C}_1 \times M_1 \boldsymbol{V}_1^{(t)} + \boldsymbol{\mathcal{I}}_1 \boldsymbol{\Omega}_1^{(t)} &= \boldsymbol{C}_1 \times M_1 \boldsymbol{V}_1^{(t+\delta t)} + \boldsymbol{\mathcal{I}}_1 \boldsymbol{\Omega}_1^{(t+\delta t)} \\ \boldsymbol{C}_2 \times M_2 \boldsymbol{V}_2^{(t)} + \boldsymbol{\mathcal{I}}_2 \boldsymbol{\Omega}_2^{(t)} &= \boldsymbol{C}_2 \times M_2 \boldsymbol{V}_2^{(t+\delta t)} + \boldsymbol{\mathcal{I}}_2 \boldsymbol{\Omega}_2^{(t+\delta t)} \quad . \end{aligned} \tag{4}$$

Finally, one also has the linear momentum balance for the two aggregates

$$M_1 \boldsymbol{V}_1^{(t)} + M_2 \boldsymbol{V}_2^{(t)} = M_1 \boldsymbol{V}_1^{(t+\delta t)} + M_2 \boldsymbol{V}_2^{(t+\delta t)}, \tag{5}$$

where M_i is the mass of A_i. Equations 1, 2, 3, 4 and 5 provide 12 equations for 12 unknowns $\{\boldsymbol{V}_1^{(t+\delta t)}, \boldsymbol{V}_2^{(t+\delta t)}, \boldsymbol{\Omega}_1^{(t+\delta t)}, \boldsymbol{\Omega}_2^{(t+\delta t)}\}$. The case of adhesion requires a different approach and will be presented shortly.

3. Variable restitution. In this section, a model is presented to estimate the unknown coefficient of restitution that appears in the equations. An average measure $\boldsymbol{F}^{avg}$ of the force involved in the impact over the duration of impact is $\boldsymbol{F}^{avg} = \frac{\boldsymbol{P}}{\delta t}$, where $\boldsymbol{P}$ is impulse. The normal component of this average force is given by $F_{nor}^{avg} = \boldsymbol{F}^{avg} \cdot \boldsymbol{n} = \frac{\boldsymbol{P} \cdot \boldsymbol{n}}{\delta t} = \frac{P_{nor}}{\delta t}$. An average contact pressure p^{avg} is defined by $p^{avg} = \frac{|F_{nor}^{avg}|}{A}$, where A is a measure of the contact area averaged over the impact duration. It is assumed that the maximum value of pressure over the duration of impact is $p = 2p^{avg}$.

A criterion was proposed by Nesterenko et al. [1994], according to which adhesion of two surfaces occurs when $p > 2H$, where H is the Vickers hardness of the material. A relationship between the contact pressure and the coefficient of restitution is provided by a linear interpolation model between elastic ($e = 1$) and adhesive ($e = 0$) conditions:

$$e = \max\{1 - \frac{p}{2H}\,,\, 0\} = \max\left\{1 - \frac{|P_{nor}|}{HA\delta t}\,,\, 0\right\} \quad . \tag{6}$$

To conduct computations, the contact area A and the duration δt of impact are needed. One would expect that as the impact is more severe, by which it is meant that e gets smaller, the contact area increases under pressure. Therefore, A is taken to be a decreasing function of e. It is assumed that A is a function of e only, scaled by a geometrical factor ϕ. A linear relation for A in terms of e is used, which was proposed by Zohdi [2003] based on the experiments of Nesterenko et al. [1994]:

$$A = (A_o + (A_f - A_o)(1 - e))\,\phi \quad , \tag{7}$$

where A_o and A_f are given coefficients. If the impact of two aggregates A_1 and A_2 occurs through sphere s_1 of A_1, and sphere s_2 of A_2, the geometry factor is defined to be $\phi = \pi\left(\min\{r_1, r_2\}\right)^2$, which is simply a scale that sets the magnitude of the contact area. For the impact of the two aggregates, the impact duration δt is on the order of $\frac{2\min\{r_1,r_2\}}{V^{avg}}$ where $V^{avg} = \frac{\left|(V_2^c)_{nor}^{(t+\delta t)} - (V_1^c)_{nor}^{(t+\delta t)}\right| + \left|(V_2^c)_{nor}^{(t)} - (V_1^c)_{nor}^{(t)}\right|}{2} = \frac{(1+e)\left|(V_2^c)_{nor}^{(t)} - (V_1^c)_{nor}^{(t)}\right|}{2}$. In other words, it is on the order of time it takes to compress and decompress the radius of the smaller sphere. If one also uses a scale factor ζ, the impact duration is given by

$$\delta t = \frac{2\zeta\min\{r_1, r_2\}}{(1+e)\left|(V_2^c)_{nor}^{(t)} - (V_1^c)_{nor}^{(t)}\right|} = \frac{2\zeta\min\{r_1, r_2\}}{(1+e)\left|(v_2)_{nor}^{(t)} - (v_1)_{nor}^{(t)}\right|} \quad . \tag{8}$$

If P_{nor} were known, one would be able to evaluate e through equation 6. However, one has $P_{nor} = M_1\left(\boldsymbol{V}_1^{(t+\delta t)} - \boldsymbol{V}_1^{(t)}\right)\cdot\boldsymbol{n} = -M_2\left(\boldsymbol{V}_2^{(t+\delta t)} - \boldsymbol{V}_2^{(t)}\right)\cdot\boldsymbol{n}$, which is in terms of e since post impact velocities depend on e. In other words, the value of e requires the solution of a nonlinear equation which can be solved, e.g., using fixed point iterations.

4. Adhesion. When the coefficient of restitution e is zero, the colliding bodies will adhere to each other (Figure 2). Upon merging, the two bodies form one body, and the bodies will have equal post-impact angular velocities, under the assumption of negligibly small deformations. Using these, one can compute the mass M_3, position $\boldsymbol{R}_3$ of the center of mass, and the inertia matrix $\boldsymbol{\mathcal{I}}_3$ of the new body. Then, it follows directly from conservation of linear and angular momentum that

$$\begin{aligned} M_3\boldsymbol{V}_3^{(t+\delta t)} &= M_1\boldsymbol{V}_1^{(t)} + M_2\boldsymbol{V}_2^{(t)} \\ \boldsymbol{\mathcal{I}}_3\boldsymbol{\Omega}_3^{(t+\delta t)} &= \boldsymbol{\mathcal{I}}_1\boldsymbol{\Omega}_1^{(t)} + \boldsymbol{\mathcal{I}}_2\boldsymbol{\Omega}_2^{(t)} + \boldsymbol{R}_3^1 \times M_1\boldsymbol{V}_1^{(t)} + \boldsymbol{R}_3^2 \times M_2\boldsymbol{V}_2^{(t)} \quad , \end{aligned} \tag{9}$$

where $\boldsymbol{R}_3^i = \boldsymbol{R}_i - \boldsymbol{R}_3$. In the case of adhesion, these equations provide 6 equations for the 6 post-impact unknowns $\{\boldsymbol{V}_3^{(t+\delta t)}, \boldsymbol{\Omega}_3^{(t+\delta t)}\}$.

5. Restructuring. It is assumed that restructuring of an aggregate takes place through disintegration into its constituent spheres. The criterion for debonding of a sphere from its aggregate is as follows. Using previous assumptions, the maximum force that acts on a sphere s_i of an aggregate is $\boldsymbol{F}_i = 2F_i^{avg}$, where $F_i^{avg} = \frac{m_i}{\delta t}(\boldsymbol{v}_i^{(t+\delta t)} - \boldsymbol{v}_i^{(t)})$ and m_i is mass of s_i. This force is applied to s_i by the N neighboring spheres it is in contact with. To decide if this sphere gets debonded from its neighbors, one checks if

$$\sigma_i^{avg} = \frac{\|\boldsymbol{F}_i\|}{A_i} > \sigma_u \quad ,$$

where A_i is defined as $A_i = \sum_{\beta=1}^{N} A_i^{\beta}$. In these equations, $A_i^{\beta}(= A_f)$ denotes the area of contact between s_i and its β-th neighboring sphere. Essentially, one compares a stress σ_i^{avg}, averaged over an area A_i, to the ultimate strength σ_u of the material. This criterion estimates that either all the bonds between a sphere and its neighbors break, or none of them break. One needs to be able to form new clusters of spheres out of an aggregate of spheres after debonding occurs, and calculate associated properties, such as velocities, with each of these clusters. The algorithm developed for this purpose sequentially checks neighboring spheres of debonded spheres, and clusters together those that are still bonded to each other (Figure 2).

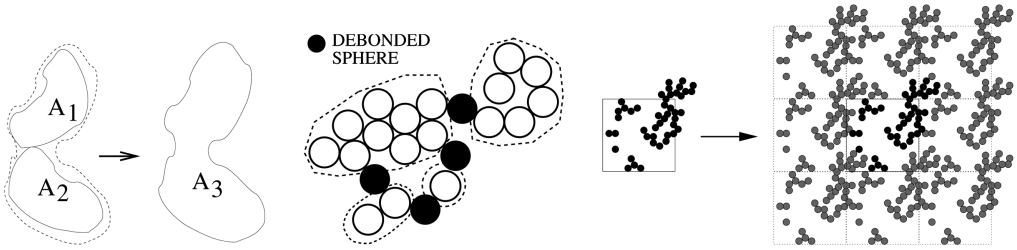

Figure 2: LEFT: Formation of a new aggregate from two aggregates. MIDDLE: An aggregate may need to be restructured after a collision. RIGHT: Periodic boundary conditions in two dimensions, where the volume element is surrounded by similar imaginary ones.

6. Numerical Experiments.

Consider the one dimensional impact of a particle with an aggregate of N particles, both travelling at the same speed, and assume all particles have the same radius. If the velocity required for adhesion of the particle to the aggregate is denoted by V_{stick} and the velocity required to debond any particle of the aggregate with one neighbor is denoted by V_{break}, the model presented can be used to calculate $V_{stick} = \sqrt{\frac{N+1}{2N}} V_{min}$ and $V_{break} = \sqrt{\frac{N+1}{4} Q_h} V_{min}$, where $Q_h = \frac{\sigma_u}{H}$, and $V_{min} = \sqrt{\frac{3\zeta H A_f}{4\rho}}$ is the minimum velocity required for bonding of two particles ($N = 1$). It follows that for a given value of the ratio $\frac{\sigma_u}{H}$, there is a critical aggregate size N' at which $V_{break} = V_{stick}$. Below this critical size ($N < N'$), $V_{break} < V_{stick}$ and all collisions will lead to disintegration of the aggregate, whenever the impacting particle adheres to the

aggregate. In other words, the aggregate will not be stable in size, and there will either be no further agglomeration or the aggregate will get smaller. Above this critical size ($N > N'$), $V_{break} > V_{stick}$ so agglomeration is stable in size. [2] In this section, numerical experiments that investigate this aspect of granular flows are presented.

A representative volume element from a granular flow is constructed by randomly packing N_s spherical particles of radius R into a cube with dimension L, at a volume fraction $Q_v = \frac{4\pi r^3}{3}\frac{N_s}{L^3}$, each with a randomly oriented velocity of magnitude $V_o = Q_o V'_{min}$. Here, $V'_{min} = \sqrt{\frac{3\zeta H A_f}{2\rho}}$ is the minimum velocity required for adhesion of a particle impacting a surface, and $V'_{min} = \sqrt{2}V_{min}$ so that $Q_o \geq 1/\sqrt{2}$ is needed for agglomeration. Periodic boundary conditions are used, with a scheme that allows for interaction across the boundaries of the volume element (Figure 2). The time step is automatically adjusted at the beginning of the simulation to $\Delta t = \frac{1}{20}\frac{r}{V_o}$. The simulation is run until the total kinetic energy decays by a factor $Q_k \approx 10^{-4}$, which is chosen so that there is little aggregation or restructuring after that time in simulation. Algorithmic details for adhesion, restructuring and implementation of boundary conditions can be found in the thesis of Temizer [2004].

To characterize agglomeration within the granular flow, the history of $Q_a = \frac{N_a}{N_s}$ is tracked, where N_a is the number of particles that are bonded to another particle. Although Q_a provides information about the percentage of agglomeration, it does not provide information about the size of aggregates. To characterize the size of agglomeration, the history of $Q_b = \frac{N_b}{N_s}$ is tracked, where N_b is the number of particles in the aggregate with largest number of particles. The time, t, is non-dimensionalized to $T = t\frac{V_o}{d_o}$, where $d_o = \frac{L}{(NQ_v)^{1/3}}$ is a measure of the distance between particles in the initial configuration (t=0). Making use of the example at the beginning of this section, it is concluded that the key control parameters for the simulations are $Q_o = \frac{V_o}{V'_{min}}$ and $Q_h = \frac{\sigma_y}{H}$. For a given particle size and volume fraction, N_s is continuously increased (together with L) until histories of Q_a and Q_b start showing clear trends for variations in Q_o and Q_h. For the range of material parameters and dense granular flows considered, where $0.1 \leq Q_v \leq 0.3$, $N_s = 1000$ was sufficient.

To demonstrate typical results, consider following variable values: $L = 2 \times 10^{-3}\,\mathrm{m}$, $\mu = 0.3$, $A_o = 0.1$, $A_f = 0.6$, $\zeta = 0.0004$, $\rho = 6000\,\mathrm{kg/m^3}$, $H = 400\,\mathrm{MPa}$, $TOL_e = 0.1$, $Q_v = 0.2$. Results for variations in Q_o (keeping $Q_h = 0.5$ constant, and using the same initial packing) are given in Figure 3. There is little aggregation for $Q_o < 4$, where the agglomerates fail to reach a critical size, and therefore they disintegrate. However, as Q_o increases, agglomerates with more than 300 particles form, and they remain stable in size until the kinetic energy decays to a point where no more adhesion or restructuring occurs. As Q_o is further increased, the size of the agglomerates grow in size, to as large as $Q_b = 0.8$. The transition from unstable agglomeration to stable agglomeration is at $Q_o = 4$ for this example, where two agglomerates with 267 and

[2] It is noted that materials typically satisfy $Q_h \leq 1$. Using this, it is observed that for $N \geq 2$, $V_{stick} < V_{min}$ and $V_{break} < V_{min}$ are possible, i.e. adhesion and restructuring of aggregates can occur for velocities less than the critical velocity for adhesion of two particles.

Figure 3: History of aggregation for various $Q_o = \frac{V_o}{V'_{min}}$ for constant $Q_h = \frac{\sigma_u}{H} = 1/2$.

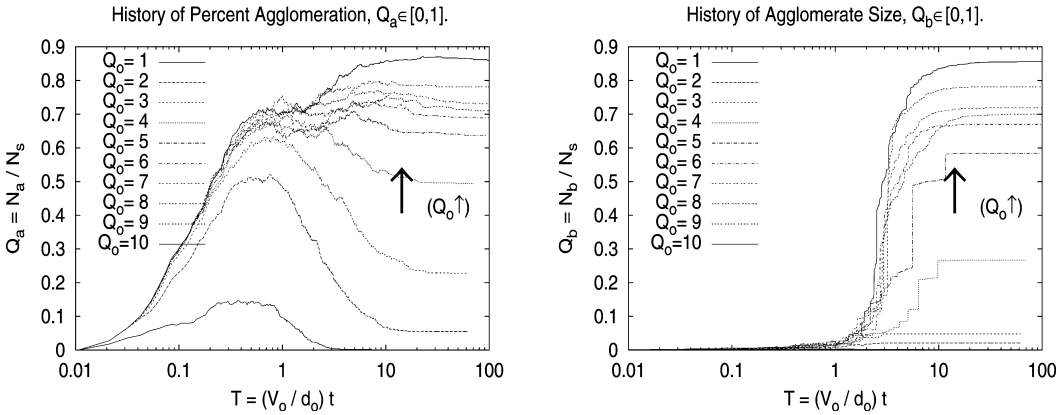

177 particles formed, and half of the particles remained free. The effect of Q_h on this transition is shown in Figure 4, where variations in Q_h (keeping $Q_o = 4$ constant, and using the same initial packing) are considered. As Q_h decreases, it becomes harder and harder for the particles to remain bonded to each other. The size of aggregates decreases, and they eventually become unstable in size, so the simulation ends with unsuccessful agglomeration. This is expected since the example at the beginning of this section had demonstrated that the critical size of aggregates increases with decreasing Q_h. Therefore, to keep the size of the aggregates the same as Q_h decreases, Q_o must be increased.

Figure 4: History of aggregation for various $Q_h = \frac{\sigma_u}{H}$ for constant $Q_o = \frac{V_o}{V'_{min}} = 4$.

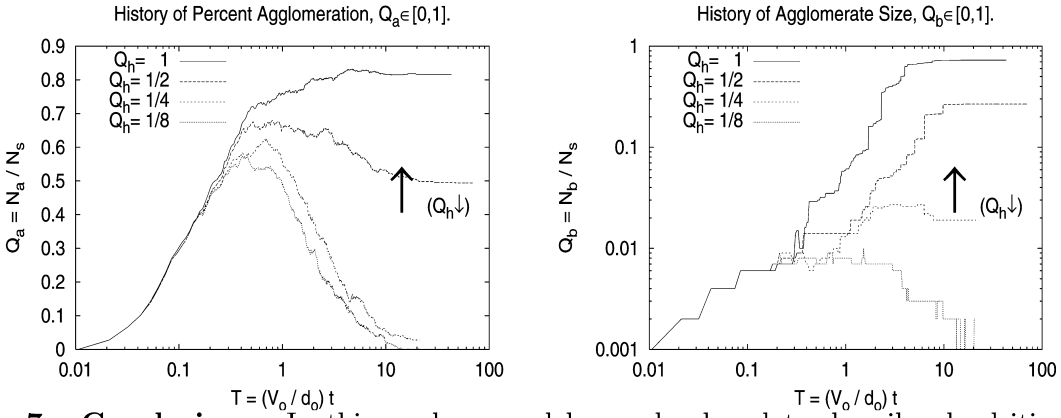

7. Conclusions. In this work, a model was developed to describe dendritic agglomeration in dense microscale granular flows. In order to isolate the mechanical bonding effects, electrical and gravitational forces were excluded from the analysis. It was shown that there are two key control parameters for agglomeration in such granular flows: (i) Q_o, the ratio of initial velocity magnitude to the critical velocity magnitude,

below which agglomeration does not occur, and (ii) Q_h, the ratio of material strength to hardness, which characterizes the relative ease with which particles will adhere or aggregates will disintegrate. If Q_h decreases, it becomes harder for particles to remain bonded, and Q_o must be larger to produce agglomerates that are stable in size. Otherwise, the energy of the system is dissipated through collisions that result in agglomerates which quickly disintegrate into their constituent particles. The inclusion of attractive and repulsive forces that exist in various forms through various scales of granular growth, as well as thermochemical effects. The inclusion will allow more degrees of freedom in terms of variation of granular flow conditions, and is the subject of current research.

References

W. Benz. Impact simulations with fracture. 1. method and tests. *Icarus*, 107:98–116, 1994.

J. Blum and G. Wurm. Impact simulations on sticking, restructuring, and fragmentation of preplanetary dust aggregates. *Icarus*, 143:138–146, 2000.

A. Chokshi, A. G. G. M. Tielens, and D. Hollenbach. Dust coagulation. *The Astrophysical Journal*, 407:806–819, 1993.

C. Dominik and A. G. G. M. Tielens. The physics of dust coagulation and the structure of dust aggregates in space. *The Astrophysical Journal*, 480:647–673, 1997.

R. H. Huijser, E. G. Van der Sar, and R. Schelling. Cosmic dust aggregation in microgravity flight report of the codag module on maser 8. In *Proc. 14th ESA Symposium on European Rocket and Balloon Programmes and Related Research*, pages 511–516, Potsdam, Germany, September 1999.

V. F. Nesterenko, M. A. Meyers, H. C. Chen, and J. C. LaSalvia. Controlled high rate localized shear in porous reactive media. *Applied Physics Letters*, 65 (24):3069–3071, 1994.

D. C. Richardson, T. Quinn, J. Stadel, and G. Lake. Direct large-scale n-body simulations of planetesimal dynamics. *Icarus*, 143:45–59, 2000.

S. Sirono and J. M. Greenberg. Do cometesimal collisions lead to bound rubble piles or to aggregates held together by gravity? *Icarus*, 145:230–238, 2000.

I. Temizer. A computational model for aggregation in a class of granular materials. Master's thesis, University of California at Berkeley, Berkeley, California, May 2004.

S. J. Weidenschilling, D. Spaute, D. R. Davis, F. Marzari, and K. Ohtsuki. Accretional evolution of a planetesimal swarm. *Icarus*, 128:429–455, 1997.

G. Wurm, J. Blum, and J. E. Colwell. A new mechanism relevant to the formation of planetesimals in the solar nebula. *Icarus*, 151:318–321, 2001.

T. I. Zohdi. Large-scale statistical inverse computation of inelastic accretion in transient granular flows. *International Journal of Nonlinear Mechanics*, 38 (8):1205–1219, 2003.

T. I. Zohdi. Modeling and direct simulation of near-field granular flows. *The International Journal of Solids and Structures*, 42/2:539–564, 2004(a).

T. I. Zohdi. (accepted) charge-induced clustering in multifield particulate flows. *International Journal of Numerical Methods in Engineering*, 2004(b).